Supporting Information

Stimuli-Responsive Phenothiazine–Tetraphenylethylene Hybrid Luminogens: Mechano- and Piezochromic Properties with Anticancer Applications

Ramakant Gavale,[a] Siddharth Singh,[b] Faizal Khan,[a] Srija Mukherjee,[b] Jiayi Yang,[c] Guanjun Xiao*[c], Bo Zou,[c] Hem Chandra Jha*[b] and Rajneesh Misra*[a]

[a] Department of chemistry, Indian Institute of Technology Indore,

Indore 453552 (India)

E-mail: rajneeshmisra@iiti.ac.in

[b] Mehta Family School of Biosciences and Biomedical Engineering, Indian Institute of Technology Indore,

Indore 453552 (India)

hemcjha@iiti.ac.in

[c] State Key Laboratory of High Pressure and Superhard Materials, College of Physics, Jilin University, Changchun 130012 (China)

xguanjun@jlu.edu.cn

(* Corresponding author)

Contents

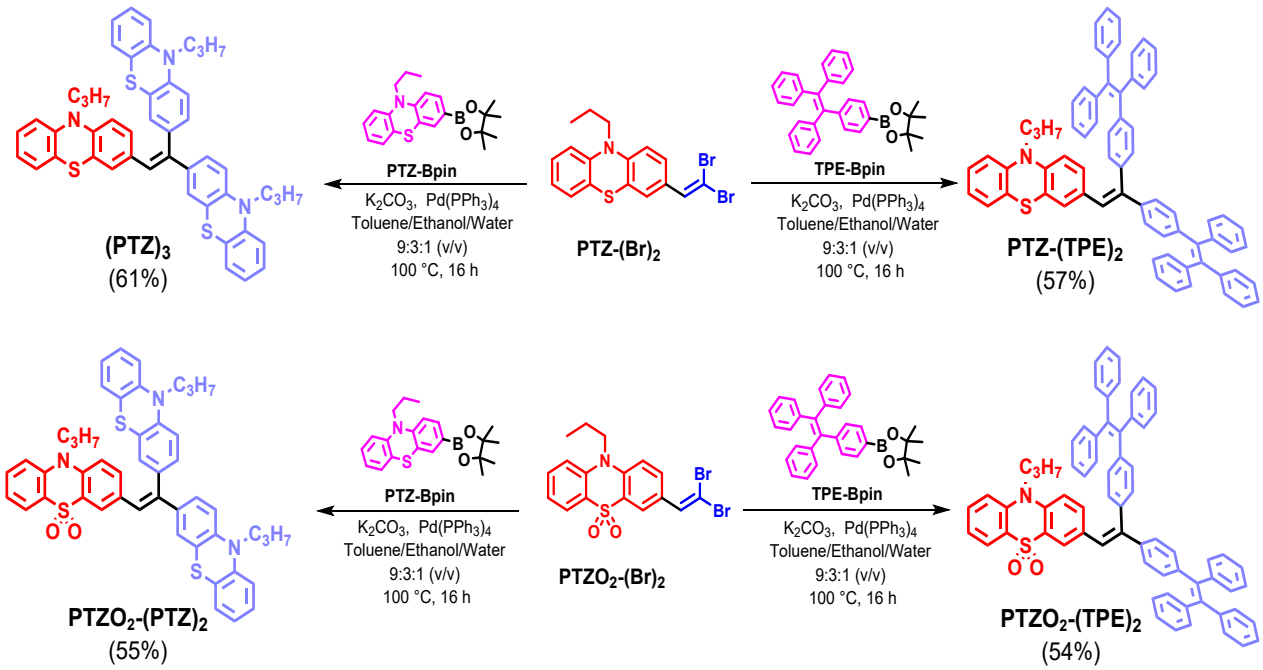

Scheme S1 Synthesis of **$(PTZ)_3$**, **$PTZO_2$-$(PTZ)_2$**, **PTZ-$(TPE)_2$**, and **$PTZO_2$-$(TPE)_2$**.

As reported in our earlier work (Ref 43), compound was synthesized by following established procedures.

Synthesis of $(PTZ)_3$

The catalyst $Pd(PPh_3)_4$ (0.040g, 0.03 mmol) was added to a well degassed solution of **PTZ-2Br** (0.150g, 0.35 mmol) and 10-propyl-3-(4,4,5,5-tetramethyl-1,3,2-dioxaborolan-2-yl)-10H-phenothiazine (**PTZ-Bpin**) (0.387g, 1.05 mmol) in toluene/ethanol/water (9:3:1, v/v) with subsequent addition of the base K_2CO_3 (0.584g,4.23 mmol). The resulting mixture was stirred and refluxed at 100 °C for 16 h under nitrogen atmosphere. After cooling, the reaction mixture was evaporated to dryness under high vacuum. Eventually, the residue was worked up with dichloromethane/water and purified by column chromatography with the eluent dichloromethane: hexane (1:3 v/v) to give yellow colour solid of **$(PTZ)_3$** in 61% Yield. ^{1}H NMR (500 MHz, $CDCl_3$, 25 °C): δ ppm 0.94-1.08 (m, 9 H), 1.72-1.94 (m, 6 H), 3.69-3.86 (m, 6 H), 6.57 (d, *J*=9 Hz, 1 H), 6.63 (s, 1 H), 6.72-6.96 (m, 12 H), 7.00-7.20 (m, 8 H).^{13}C NMR (126 MHz, $CDCl_3$, 25 °C): δ 145.22, 145.01, 144.90, 144.50, 144.41, 143.54, 138.99, 137.77, 134.13, 131.88, 129.43, 128.82, 128.38, 128.18, 127.45, 127.36, 127.17, 127.08, 126.62,

126.17, 125.40, 125.02, 124.64, 124.47, 124.44, 124.39, 123.89, 122.35, 122.32, 122.25, 115.48, 115.30, 115.18, 114.86, 114.76, 49.32, 49.21, 49.14, 20.13, 20.06, 11.42, 11.35, 11.31 ppm. HRMS (ESI): Calcd. for $C_{47}H_{43}N_3S_3$ $[M]^+$: 745.2620, Found: 745.2614.

Synthesis of $PTZO_2$-$(PTZ)_2$

The catalyst $Pd(PPh_3)_4$ (0.037g, 0.032 mmol) was added to a well degassed solution of **$PTZO_2$-2Br** (0.150g, 0.32 mmol) and 10-propyl-3-(4,4,5,5-tetramethyl-1,3,2-dioxaborolan-2-yl)-10H-phenothiazine (**PTZ-Bpin**) (0.360g, 0.98 mmol) in toluene/ethanol/water (9:3:1, v/v) with subsequent addition of the base K_2CO_3 (0.543g, 3.93 mmol). The resulting mixture was stirred and refluxed at 100 °C for 16 h under nitrogen atmosphere. After cooling, the reaction mixture was evaporated to dryness under high vacuum. Eventually, the residue was worked up with dichloromethane/water and purified by column chromatography with dichloromethane:hexane (9:1 v/v) as eluent to give yellow colour solid of **$PTZO_2$-$(PTZ)_2$** in solid 55% Yield. ^{1}H NMR (500 MHz, $CDCl_3$, 25 °C): δ ppm 0.99-1.08 (m, 9 H), 1.80-1.93 (m, 6 H), 3.79 - 3.85 (m, 4 H), 4.02 (t, *J*=7.5 Hz, 2 H), 6.77 (d, *J*=9 Hz, 2 H), 6.81 (s, 1 H), 6.83 (d, *J*=8 Hz, 1 H), 6.87-6.96 (m, 5 H), 6.99 (d, *J*=9 Hz, 1 H), 7.06-7.20 (m, 7 H), 7.22-7.25 (m, 1 H), 7.28 (s, 1 H), 7.56-7.61 (m, 1 H), 7.92 (d, *J*=2 Hz, 1 H), 8.09 (dd, *J*=8 Hz , 1.37 Hz, 1 H). ^{13}C NMR (126 MHz, $CDCl_3$, 25 °C): δ 144.99, 144.96, 144.90, 144.81, 141.04, 140.59, 138.74, 137.14, 133.14, 133.56, 133.09, 133.00, 131.79, 129.53, 128.76, 127.48, 127.23, 126.76, 126.40, 125.14, 124.77, 124.55, 124.47, 124.02, 123.75, 122.46, 122.42, 121.67, 115.80, 115.57, 115.50, 115.36, 114.94, 49.92, 49.37, 49.24, 20.14, 20.11, 20.05, 11.39, 11.35, 10.98 ppm. HRMS (ESI): Calcd. for $C_{47}H_{43}N_3O_2S_3$ $[M+Na]^+$: 800.2436, Found: 800.2410.

Synthesis of PTZ-$(TPE)_2$

The catalyst $Pd(PPh_3)_4$ (0.027g, 0.023 mmol) was added to a well degassed solution of **PTZ-2Br** (0.100g, 0.235 mmol) and 4,4,5,5-tetramethyl-2-(4-(1,2,2-triphenylvinyl)phenyl)-1,3,2-dioxaborolane (**TPE-Bpin**) (0.323g, 0.070 mmol) in toluene/ethanol/water (9:3:1, v/v) with subsequent addition of the base K_2CO_3 (0.389g, 2.82 mmol). The resulting mixture was stirred and refluxed at 100 °C for 16 h under nitrogen atmosphere. After cooling, the reaction mixture was evaporated to dryness under high vacuum. Eventually, the residue was worked up with dichloromethane/water and purified by column chromatography with dichloromethane:hexane (1:4 v/v) as eluent to give yellow colour solid of **PTZ-$(TPE)_2$** in 57% Yield. ^{1}H NMR (500 MHz, $CDCl_3$, 25 °C): δ ppm 1.01 (t, *J*=7 Hz, 3 H), 1.76-1.87 (m, 2 H), 3.77(t, *J*=7 Hz, 2 H),

6.59 (d, *J*=9 Hz, 1 H), 6.71-6.74 (m, 2 H), 6.77 (dd, *J*=9 Hz, 2 Hz, 1 H), 6.81 (d, *J*=8 Hz, 1 H), 6.87-6.95 (m, 5 H), 6.96-7.16 (m, 36 H). ^{13}C NMR (126 MHz, $CDCl_3$, 25 °C): δ 144.78, 143.83, 143.81, 143.74, 143.72, 143.66, 143.56, 142.98, 142.66, 140.99, 140.85, 140.82, 140.62, 140.43, 138.28, 138.28, 131.84, 131.77, 131.45, 131.36, 131.10, 129.65, 128.54, 128.05, 127.73, 127.67, 127.64, 127.60, 127.36, 127.13, 126.49, 126.42, 126.36, 126.16, 124.42, 123.80, 122.31, 115.24, 114.50, 49.18, 29.70, 20.11, 11.34 ppm. HRMS (ESI): Calcd. for $C_{69}H_{53}NS$ $[M+H]^+$: 928.3968, Found: 928.3971.

Synthesis of $PTZO_2$-$(TPE)_2$

The catalyst $Pd(PPh_3)_4$ (0.037g, 0.032 mmol) was added to a well degassed solution of **$PTZO_2$-2Br** (0.150g, 0.328 mmol) and 4,4,5,5-tetramethyl-2-(4-(1,2,2-triphenylvinyl)phenyl)-1,3,2-dioxaborolane (**TPE-Bpin**) (0.451g, 0.098mmol) in toluene/ethanol/water (9:3:1, v/v) with subsequent addition of the base K_2CO_3 (0.543g, 3.93 mmol). The resulting mixture was stirred and refluxed at 100 °C for 16 h under nitrogen atmosphere. After cooling, the reaction mixture was evaporated to dryness under high vacuum. Eventually, the residue was worked up with dichloromethane/water and purified by column chromatography with dichloromethane: hexane (4:1 v/v) as eluent to give cyan colour solid of **$PTZO_2$-$(TPE)_2$** in 54% Yield. ^{1}H NMR (500 MHz, $CDCl_3$, 25 °C): δ ppm 1.09 (t, *J*=7 Hz, 3 H), 1.89-2.01 (m, 2 H), 4.08 (t, *J*=7 Hz, 2 H), 6.85-7.25 (m, 41 H), 7.27-7.37 (m, 2 H), 7.60 (t, *J*=8 Hz, 1 H), 7.85 (d, *J*=2 Hz, 1 H), 8.11 (d, *J*=8 Hz, 1 H). ^{13}C NMR (126 MHz, $CDCl_3$, 25 °C): δ 143.94, 143.80, 143.71, 143.65, 143.46, 143.42, 143.28, 142.59, 141.26, 141.15, 140.85, 140.62, 140.56, 140.46, 138.89, 137.65, 133.55, 133.04, 131.96, 131.71, 131.53, 131.36, 131.23, 129.68, 127.81, 127.72, 127.66, 127.57, 126.68, 126.51, 126.46, 124.93, 124.62, 124.01, 123.77, 121.77, 115.89, 115.31,49.95, 20.22, 11.06 ppm. HRMS (ESI): Calcd. for $C_{69}H_{53}NO_2S$ $[M+K]^+$: 998.3468, Found: 998.3429.

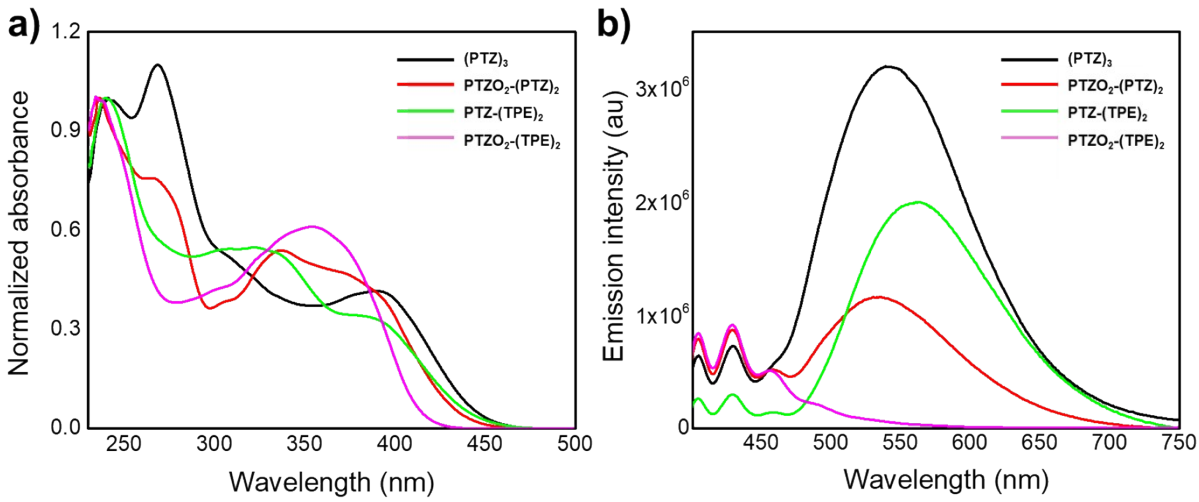

Fig. S1 (a) Normalized absorption and (b) emission spectra of tetrahydrofuran solutions (10^{-5} M) of **$(PTZ)_3$**, **$PTZO_2$-$(PTZ)_2$**, **PTZ-$(TPE)_2$**, and **$PTZO_2$-$(TPE)_2$** recorded at 25 °C (λ_{ex} = 390 nm).

Table S1 Photophysical and computational data of **$(PTZ)_3$**, **$PTZO_2$-$(PTZ)_2$**, **PTZ-$(TPE)_2$**, and **$PTZO_2$-$(TPE)_2$**.

Compounds	λ_{abs} (nm) [a] (ε (M^{-1} cm^{-1})) [a]	λ_{em} (nm) [a]	E_g^{opt} (eV)[a]	E_{HOMO}[b] (eV)	E_{LUMO}[b] (eV)	E_g[b] (eV)
$(PTZ)_3$	241 (55900), 268 (61500), 390 (23200)	539	2.78	-4.72	-1.22	3.50
$PTZO_2$-$(PTZ)_2$	236 (46100), 266 (35000), 337 (24900)	534	2.86	-4.91	-1.42	3.49
PTZ-$(TPE)_2$	240 (61900), 322 (33900), 382 (21100)	561	2.79	-4.83	-1.49	3.34
$PTZO_2$-$(TPE)_2$	234 (55300), 355 (33600)	-	2.99	-5.12	-1.64	3.48

([a]Absorption and emission were measured in tetrahydrofuran solution (10^{-5} M). [b]Values were obtained from density functional theory calculations using the Gaussian 09W program at the B3LYP/6-31G(d,p) level).

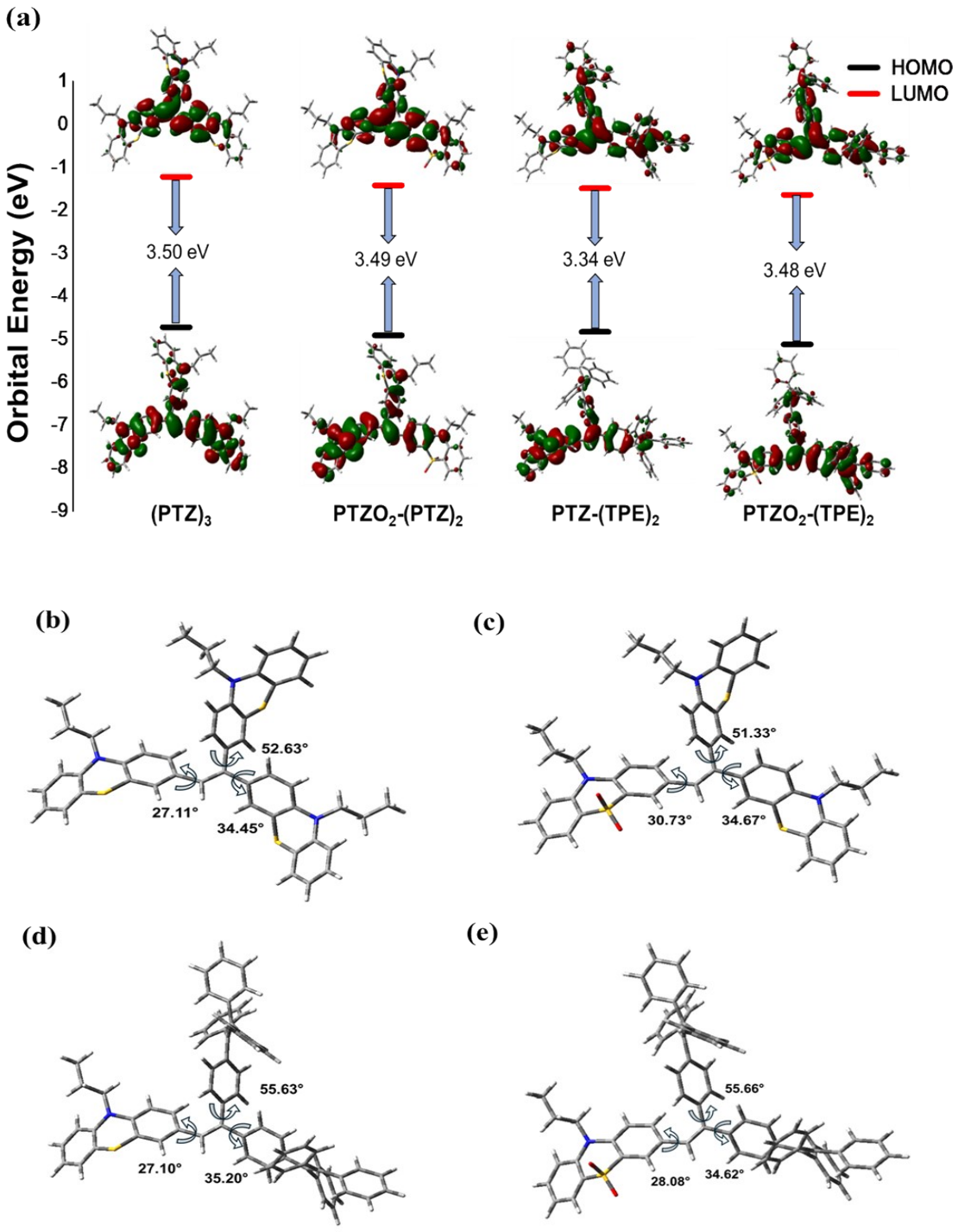

Fig. S2 a) Energy level diagram and frontier molecular orbitals of **$(PTZ)_3$**, **$PTZO_2$-$(PTZ)_2$**, **PTZ-$(TPE)_2$**, and **$PTZO_2$-$(TPE)_2$**. DFT optimized structure of b) **$(PTZ)_3$**, c) **$PTZO_2$-$(PTZ)_2$**, d) **PTZ-$(TPE)_2$**, and e) **$PTZO_2$-$(TPE)_2$** with calculated bong angles at vinylic position.

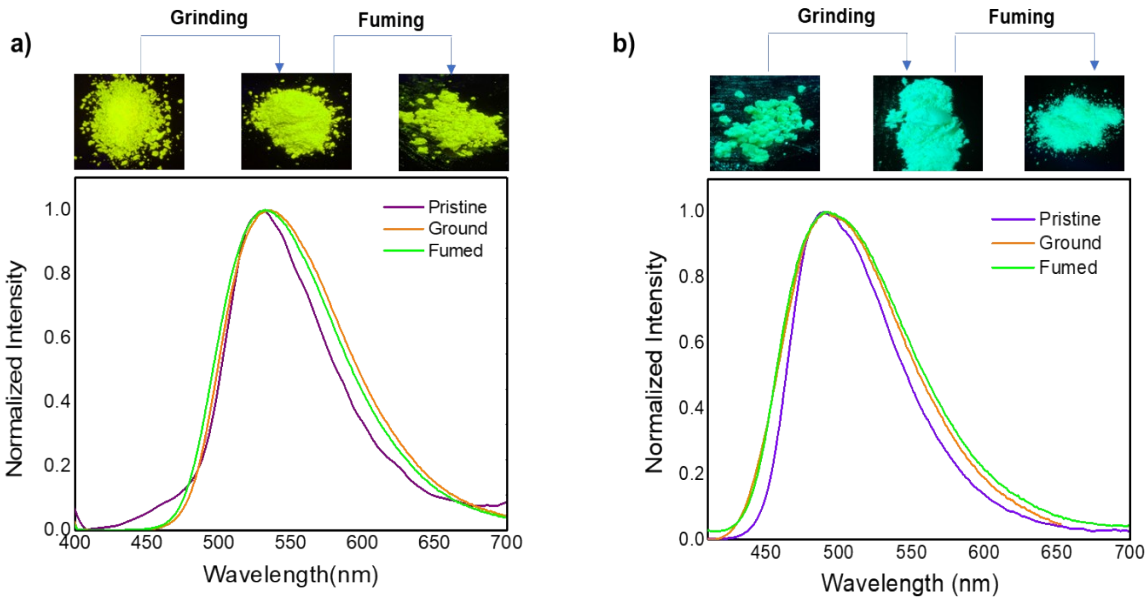

Fig. S3 Normalized emission spectra of (c) **PTZ-(TPE)$_2$** and (b) **PTZO$_2$-(TPE)$_2$** under different mechanical stimuli recorded at 25 °C (λ_{ex} = 390 nm). (Inset: fluorescence images taken under UV illumination).

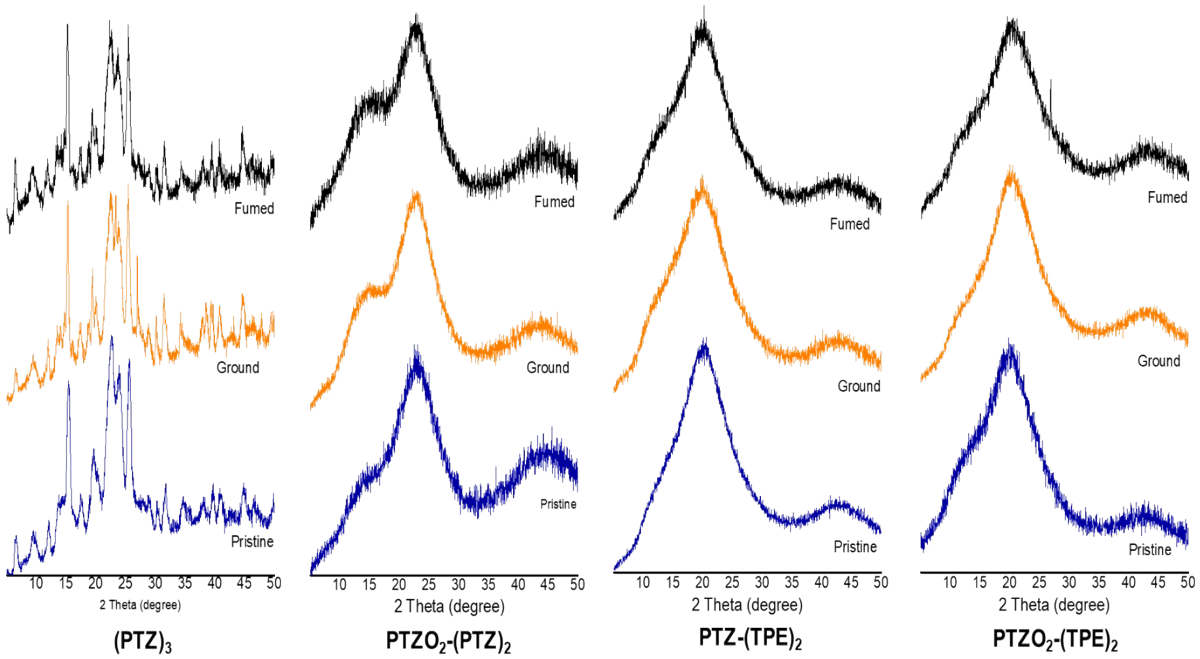

Fig. S4 PXRD patterns for the pristine, ground and fumed forms of **(PTZ)$_3$**, **PTZO$_2$-(PTZ)$_2$**, **PTZ-(TPE)$_2$**, and **PTZO$_2$-(TPE)$_2$**.

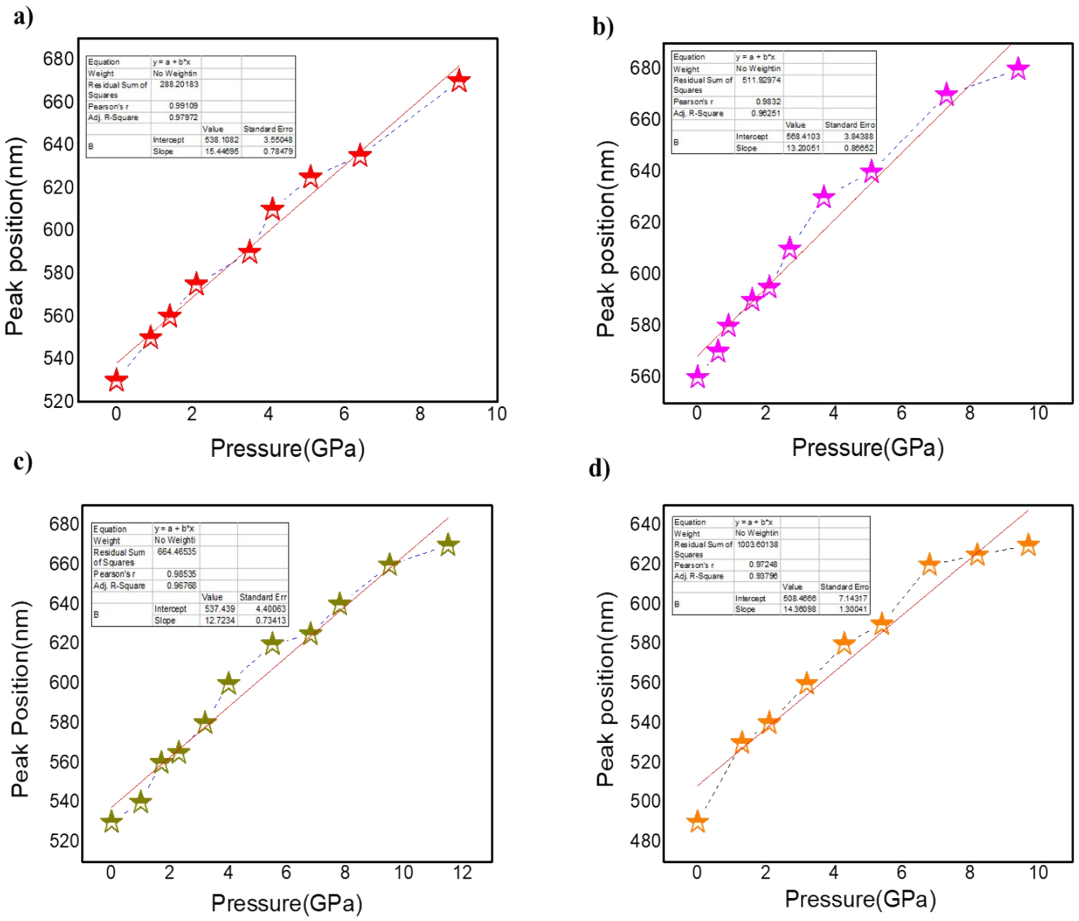

Fig. S5 The plots of emission maxima (λmax) as a function of applied pressure for compounds **$(PTZ)_3$**, **$PTZO_2$-$(PTZ)_2$**, **PTZ-$(TPE)_2$**, and **$PTZO_2$-$(TPE)_2$**.

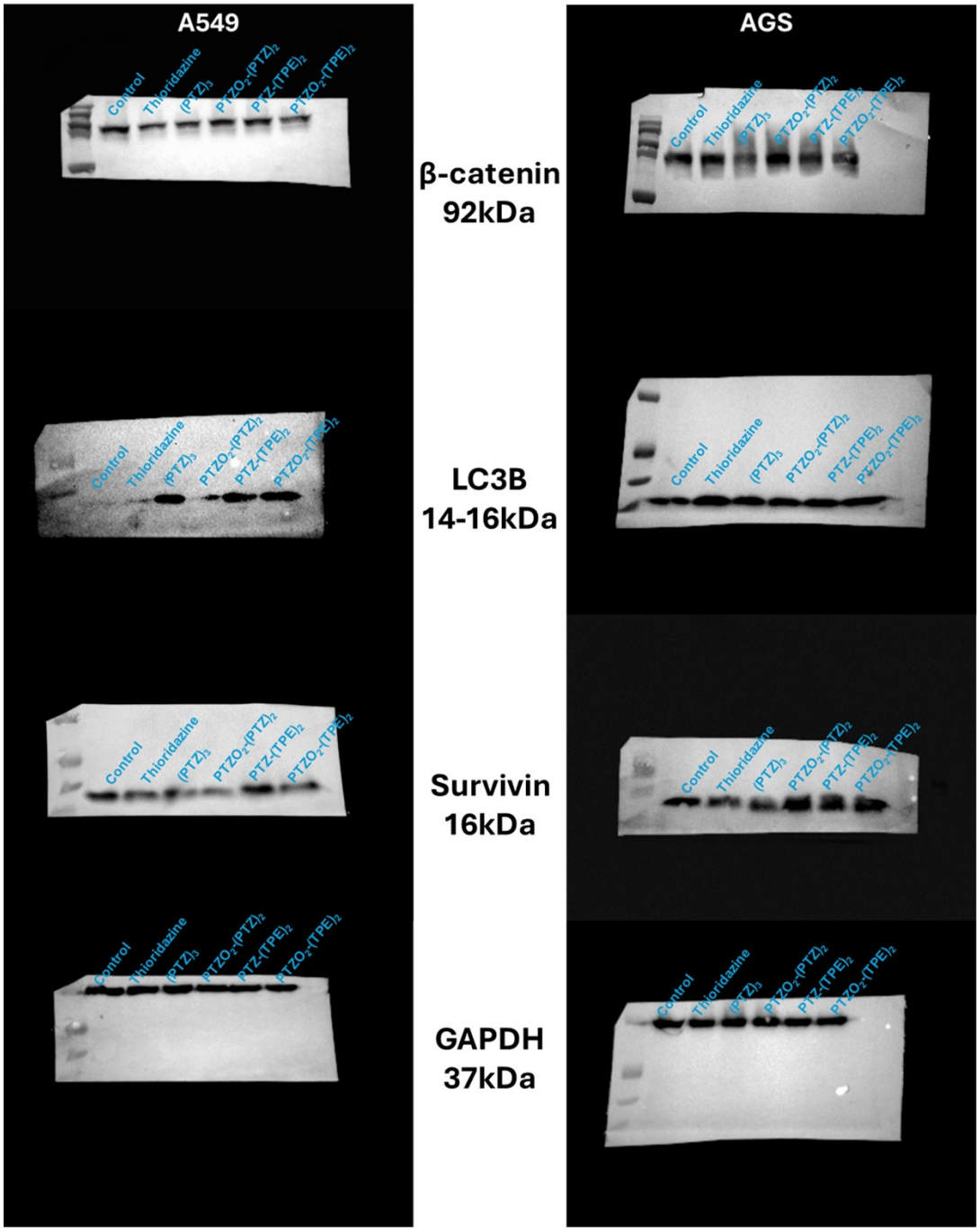

Fig. S6 Uncropped immunoblots for pathway markers in A549 and AGS cells (24 h, sub-IC dosing). (A) A549 and (B) AGS whole-cell lysates probed for β-catenin, LC3B, and Survivin; GAPDH serves as the loading control. Cells were treated for 24 h at IC_{10} concentrations (from Fig. 6 & 7) with: vehicle (Control), Thioridazine (THZ), **$(PTZ)_3$, $PTZO_2$-$(PTZ)_2$, PTZ-$(TPE)_2$, or $PTZO_2$-$(TPE)_2$.** Proteins were resolved on 10% polyacrylamide gels, transferred to nitrocellulose membrane, and detected by chemiluminescence under identical exposure settings across lanes within each blot. Images shown are uncropped membranes with sample order annotated.

Table S2 IC_{20} (80% viability) - point estimates and selectivity

Compound	A549 IC_{20} (µM)	AGS IC_{20} (µM)	HEK293 IC_{20} (µM)	SI_{20} A549/HEK	SI_{20} AGS/HEK	ΔIC_{20} (A549–HEK)	p	ΔIC_{20} (AGS–HEK)	p
$(PTZ)_3$	5.68	2.93	17.77	0.32	0.17	−12.09	0.004	−14.84	<0.001
$PTZO_2$–$(PTZ)_2$	>100[a]	7.31	33.37	>2.99	0.22	n.e.[b]	—	−26.06	<0.001
PTZ–$(TPE)_2$	45.12	30.74	9.52	4.74	3.23	+35.60	<0.001	+21.22	0.002
$PTZO_2$–$(TPE)_2$	76.98	29.90	60.30	1.28	0.50	+16.68	0.090	−30.40	0.003
Thioridazine (pos. ctrl.)	3.51	5.22	10.48	0.34	0.50	−6.97	0.011	−5.26	0.032

Notes. [a]80% viability not reached by 100 µM. [b]n.e., not estimable as a finite ΔIC_{20} because the A549 IC_{20} exceeds the top dose. Linear interpolation on mean curves, 0–100 µM; 24 h; dark.

The 24-h MTT dose–response data (0-100 µM) for A549, AGS, and HEK293 were summarized as the mean viability at each dose (n = 3). IC_{20} was defined as the concentration giving 80% viability and obtained by exact linear interpolation between the two adjacent doses bracketing 80%. To compare cancer vs. non-cancer IC_{20} values (A549 or AGS vs. HEK293), we used a nonparametric bootstrap (resampling replicates within each dose; 4,000 iterations) to compute p-values for the null hypothesis of equal IC_{20} (two-sided; p computed as $2 \times \min\{\Pr(\Delta \geq 0), \Pr(\Delta \leq 0)\}$). Bootstrap confidence procedures for dose-metrics are well established and robust at small n https://doi.org/10.1111/j.0272-4332.2004.00409.x.

The **$(PTZ)_3$** shows strong cancer selectivity at sub-lethal effect (SI_{20} = 0.32 in A549; 0.17 in AGS) with significant differences vs HEK293 (p = 0.004 and <0.001, respectively). **PTZ-$(TPE)_2$** is more toxic to HEK293 at low effect (SI_{20} > 3 in both cancers), with highly significant ΔIC_{20} (A549-HEK = +35.6 µM, p < 0.001), indicating a narrower therapeutic window near IC_{20}. $PTZO_2$-$(PTZ)_2$ appears least cytotoxic to A549 (IC_{20} > 100 µM), but active in AGS (IC_{20} ≈ 7.3 µM, p < 0.001 vs HEK293), highlighting histotype-dependent susceptibility. $PTZO_2$-$(TPE)_2$ is not different from HEK293 in A549 at IC_{20} (p = 0.090) but is significantly more active in AGS (p = 0.003). Positive control thioridazine shows expected cancer selectivity at

low effect with significant ΔIC_{20}. At IC_{20}, $(PTZ)_3$ displays clear cancer-preferring activity, consistent with literature that phenothiazines modulate redox and membrane signaling to tip apoptosis in malignant cells at sub-lethal doses. The TPE-conjugated analog **PTZ-$(TPE)_2$** shows the opposite trend, cautioning that its intrinsic cytotoxicity to non-cancer cells can dominate unless dosing is tightly controlled or combined with spatiotemporal activation (e.g., PDT). The sulfone-bridged **$PTZO_2$-$(PTZ)_2$** is weakly cytotoxic to A549 ($IC_{20} > 100$ μM) yet remains potent in AGS ($p < 0.001$), underscoring line-specific vulnerabilities.

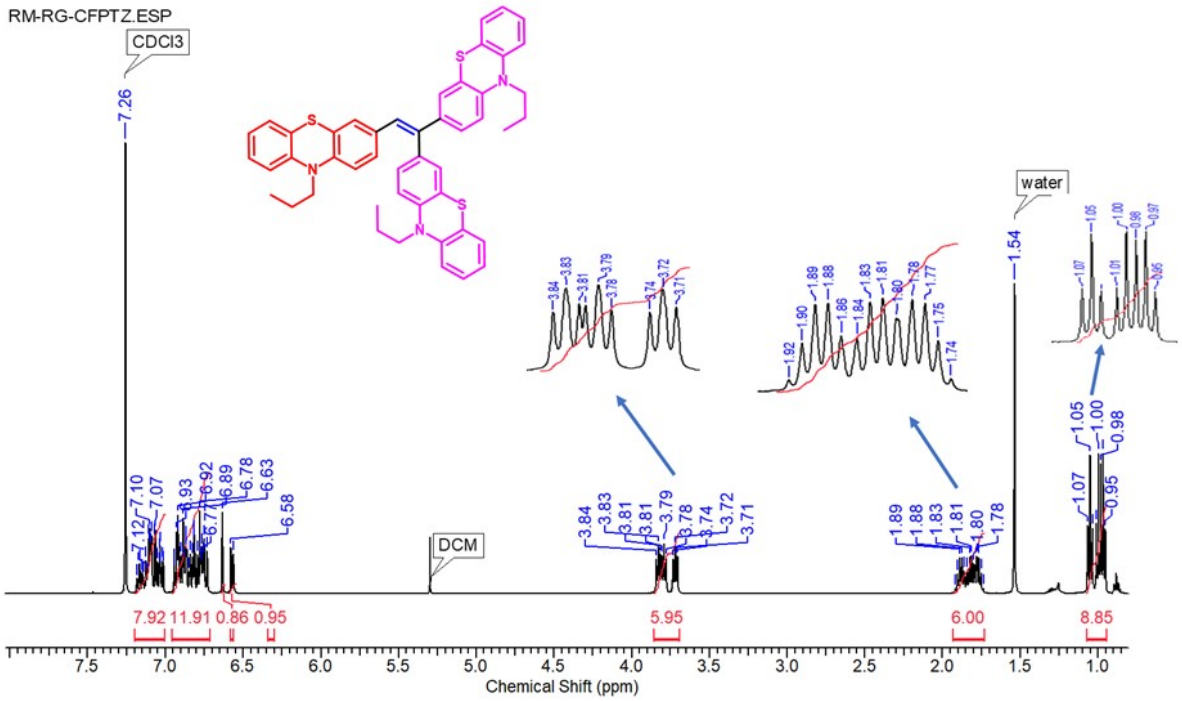

Fig. S7 ^{1}H NMR spectra of **(PTZ)$_3$** ($CDCl_3$, 500 MHz).

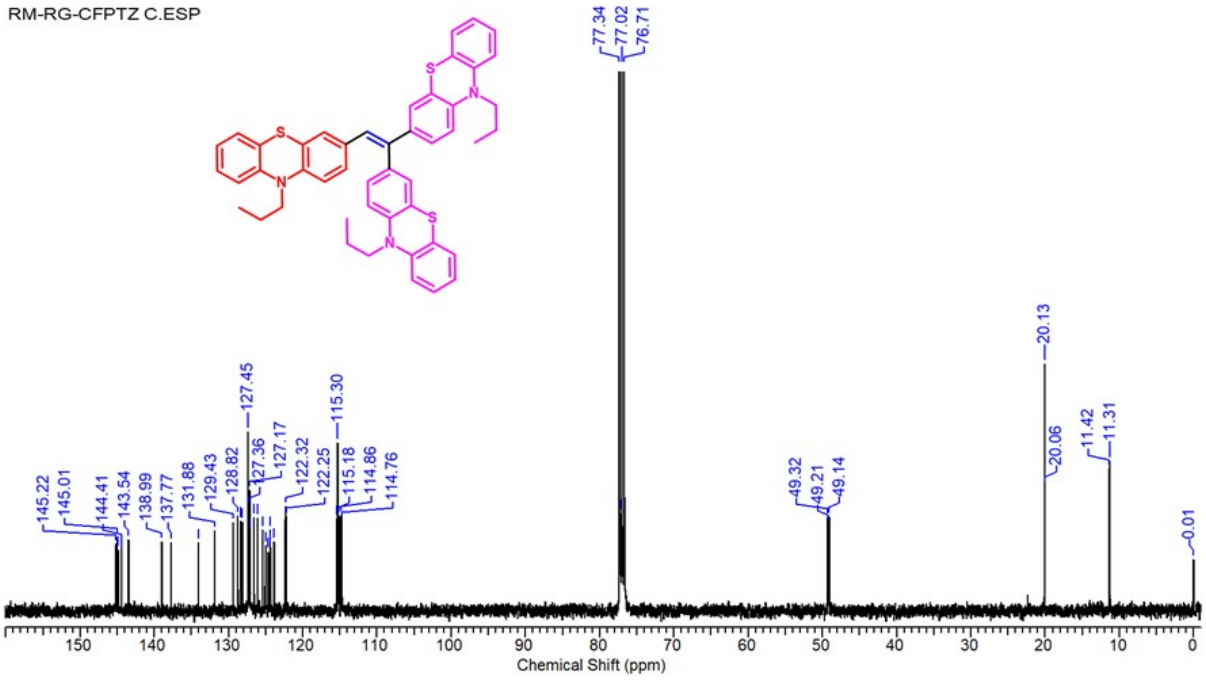

Fig. S8. ^{13}C {^{1}H} NMR spectra of **(PTZ)$_3$** ($CDCl_3$, 126 MHz).

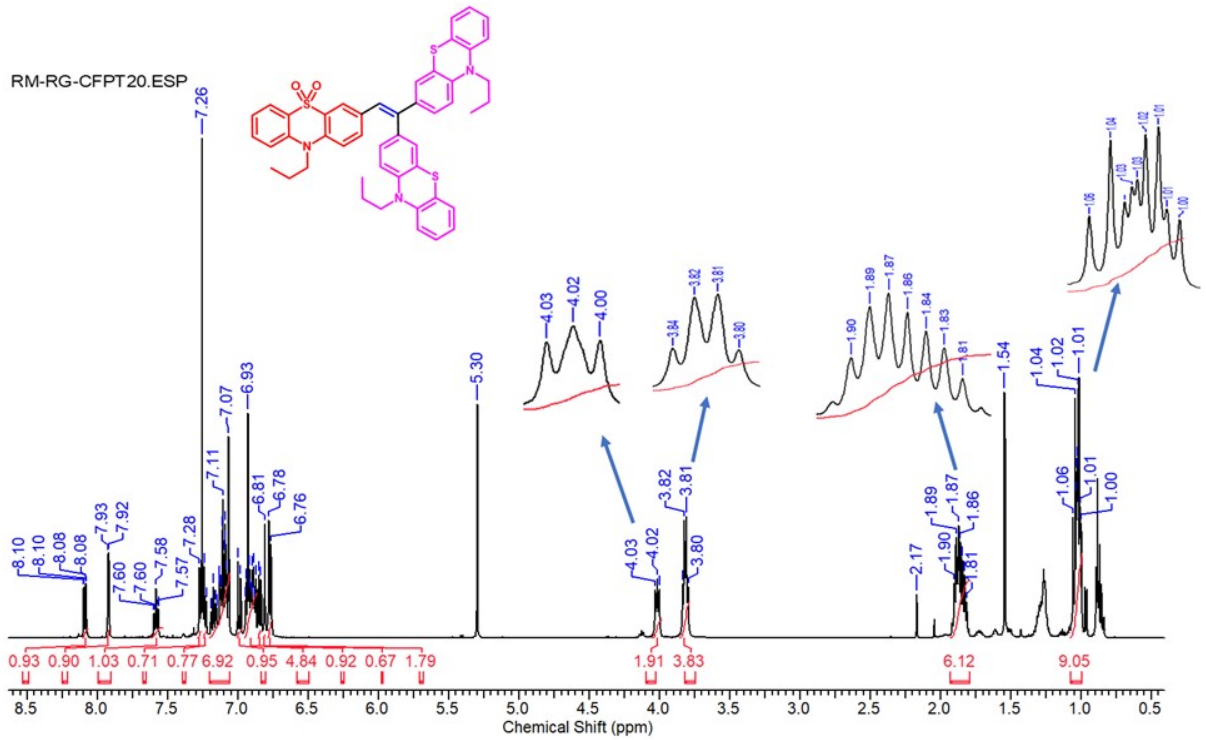

Fig. S9. ^{1}H NMR spectra of **$PTZO_2$-$(PTZ)_2$** ($CDCl_3$, 500 MHz).

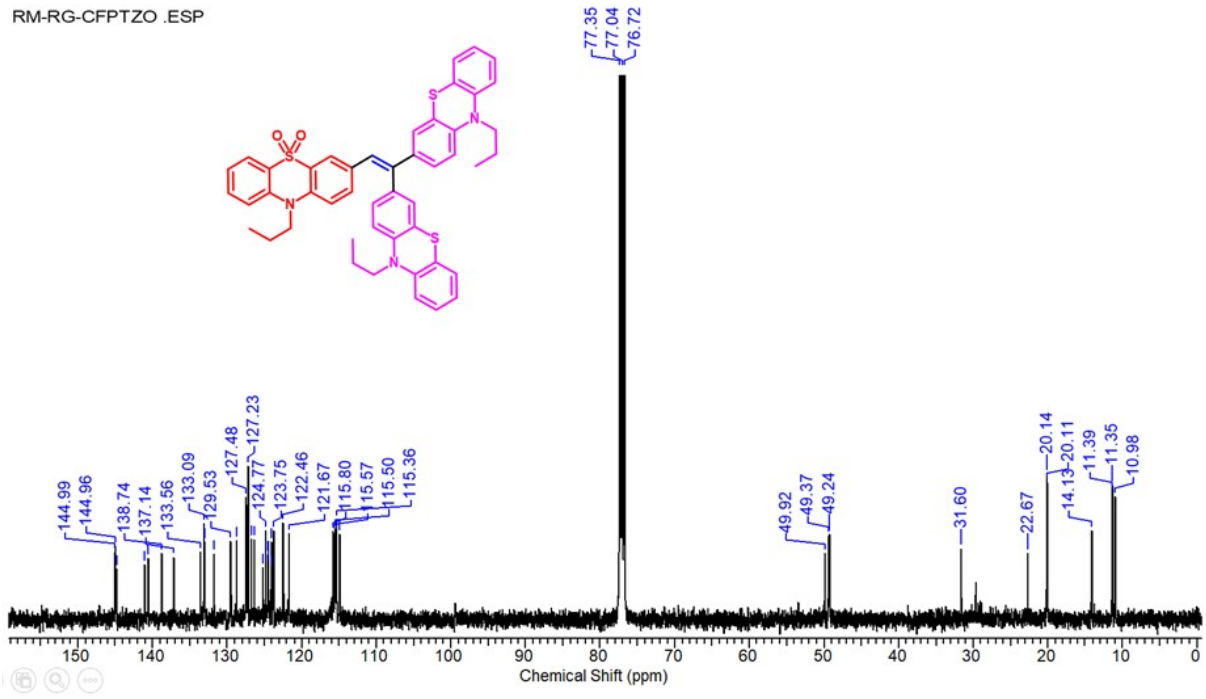

Fig. S10. ^{13}C {^{1}H} NMR spectra of **$PTZO_2$-$(PTZ)_2$** ($CDCl_3$, 126 MHz).

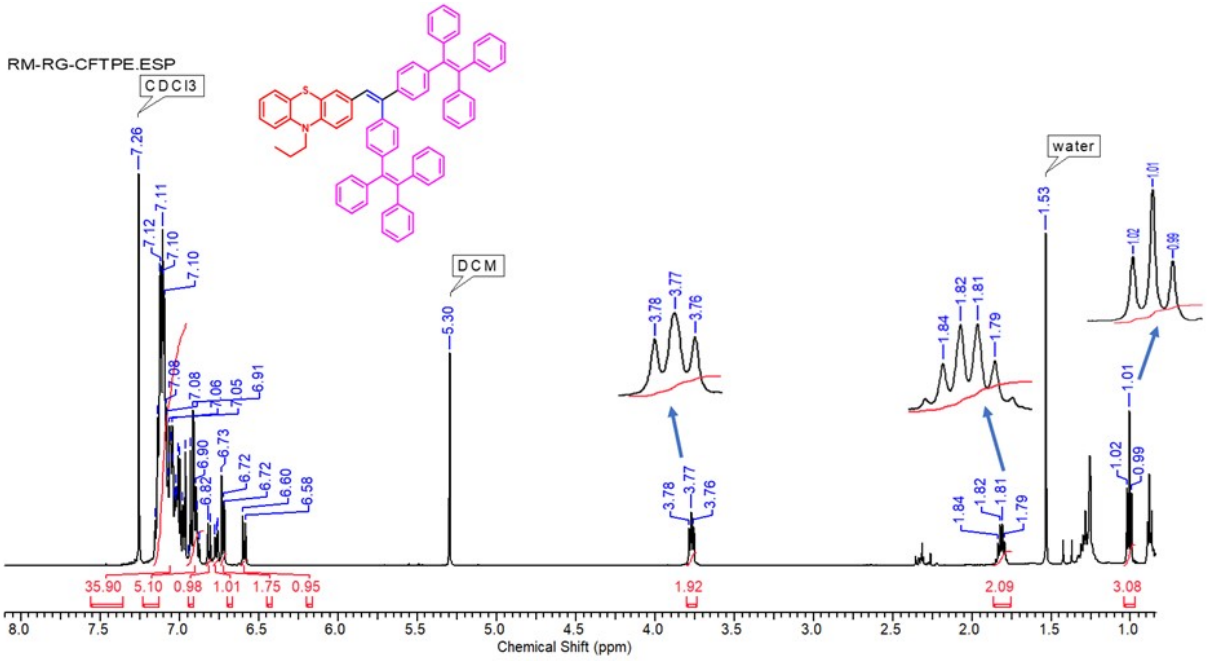

Fig. S11. ^{1}H NMR spectra of **PTZ-(TPE)$_2$** ($CDCl_3$, 500 MHz).

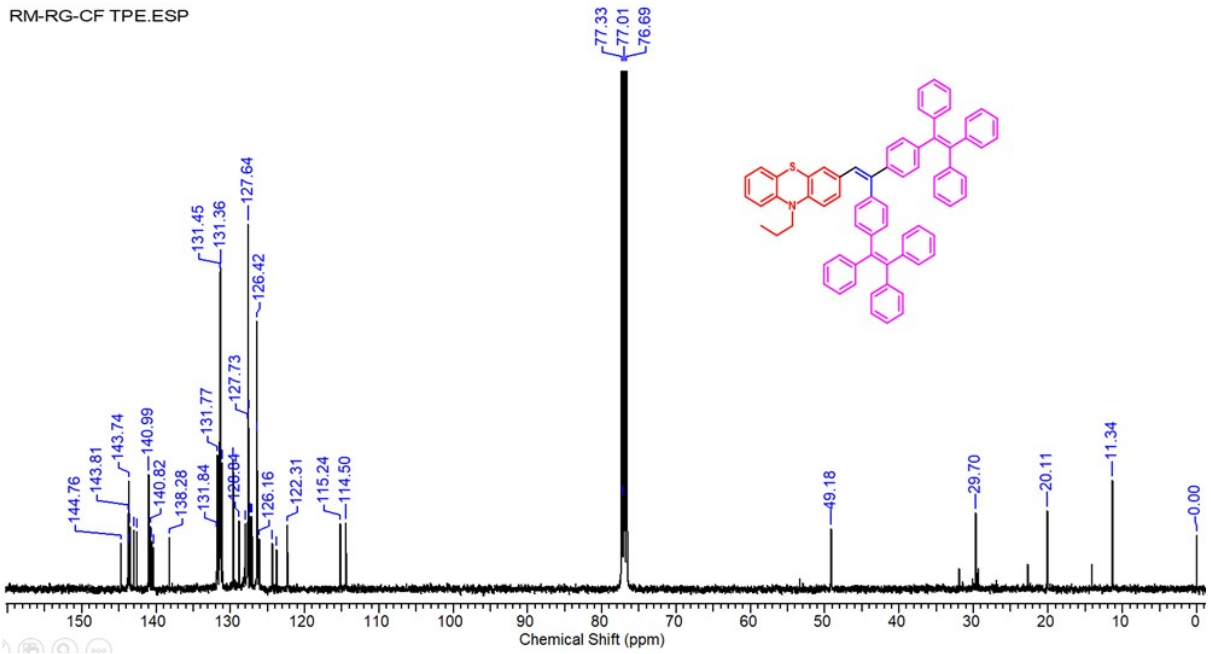

Fig. S12. ^{13}C {^{1}H} NMR spectra of **PTZ-(TPE)$_2$** ($CDCl_3$, 126 MHz).

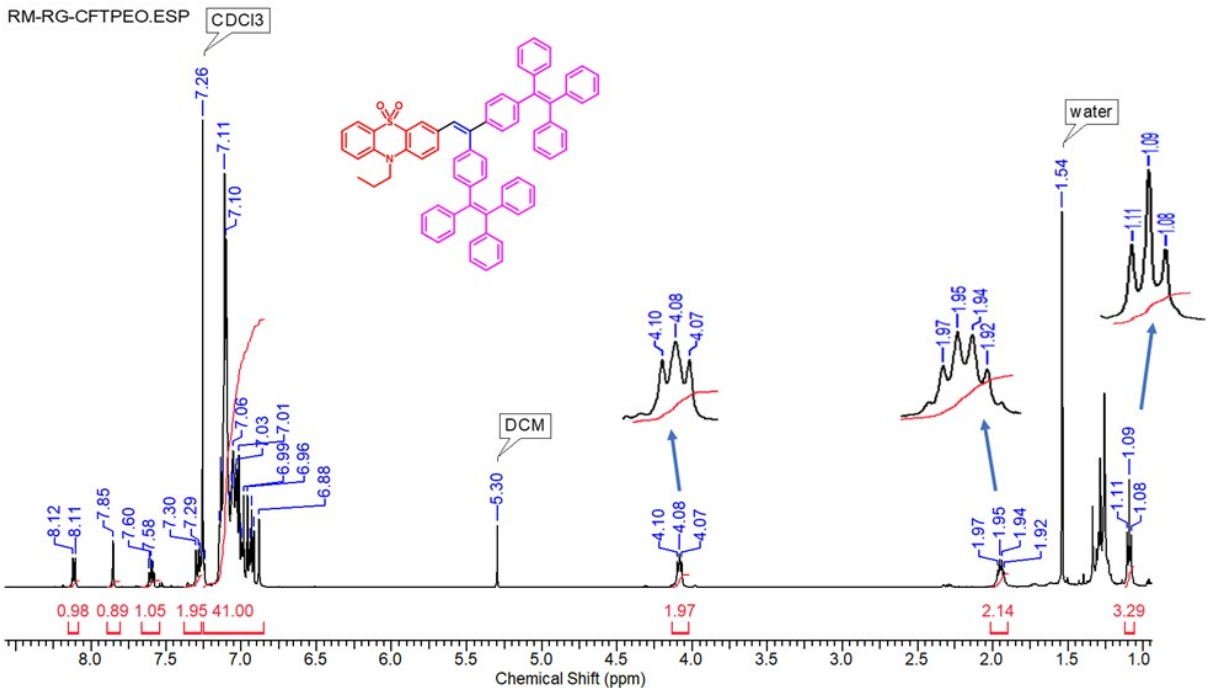

Fig. S13. ^{1}H NMR spectra of **$PTZO_2$-$(TPE)_2$** ($CDCl_3$, 500 MHz).

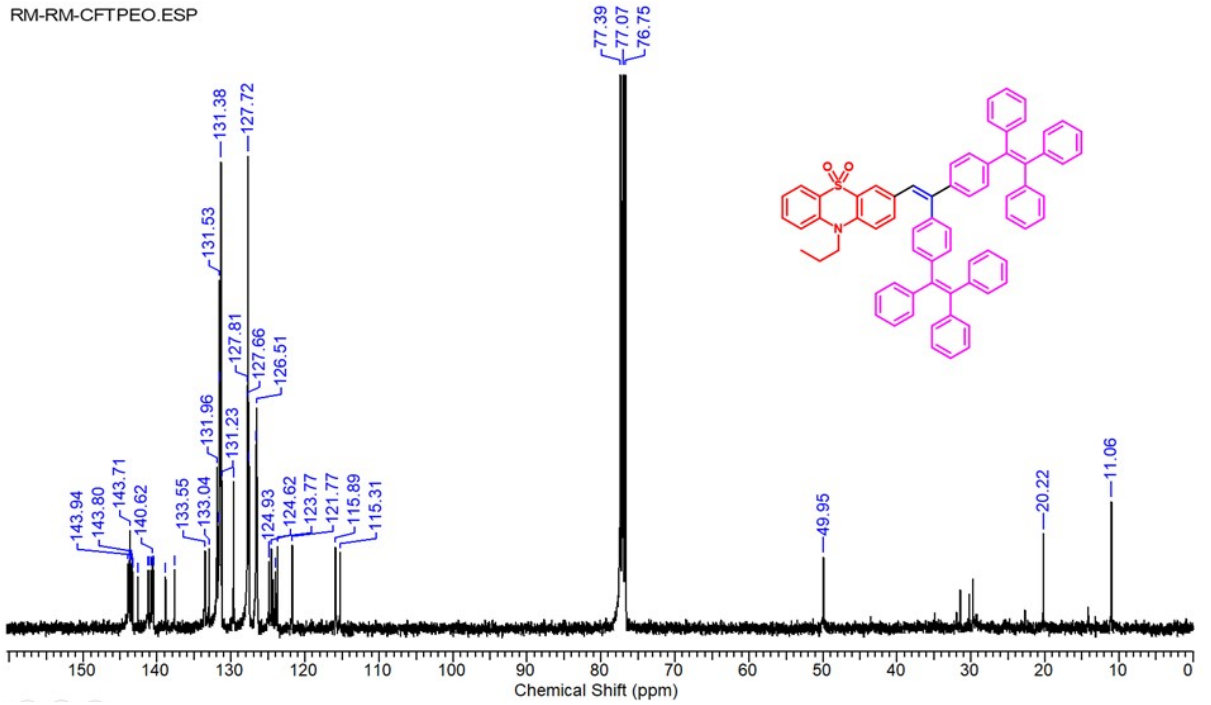

Fig. S14. ^{13}C {^{1}H} NMR spectra of **$PTZO_2$-$(TPE)_2$** ($CDCl_3$, 126 MHz).

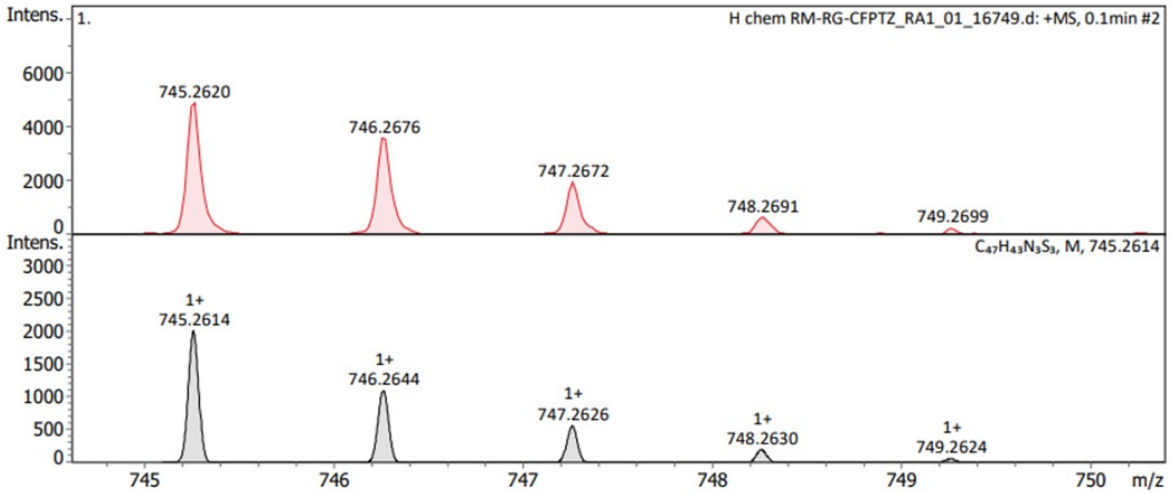

Fig. S15. HRMS of **$(PTZ)_3$**.

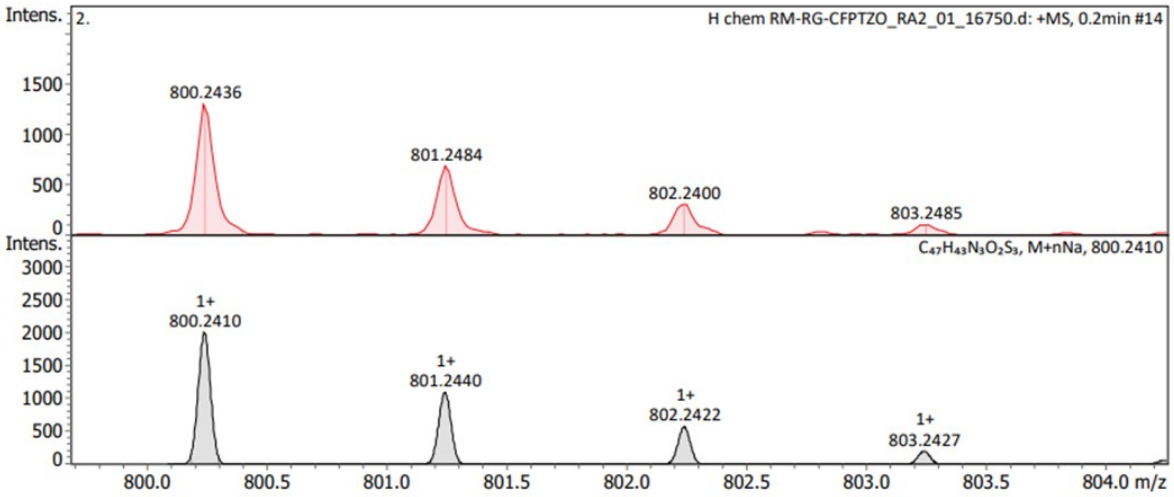

Fig. S16. HRMS of **$PTZO_2$-$(PTZ)_2$**.

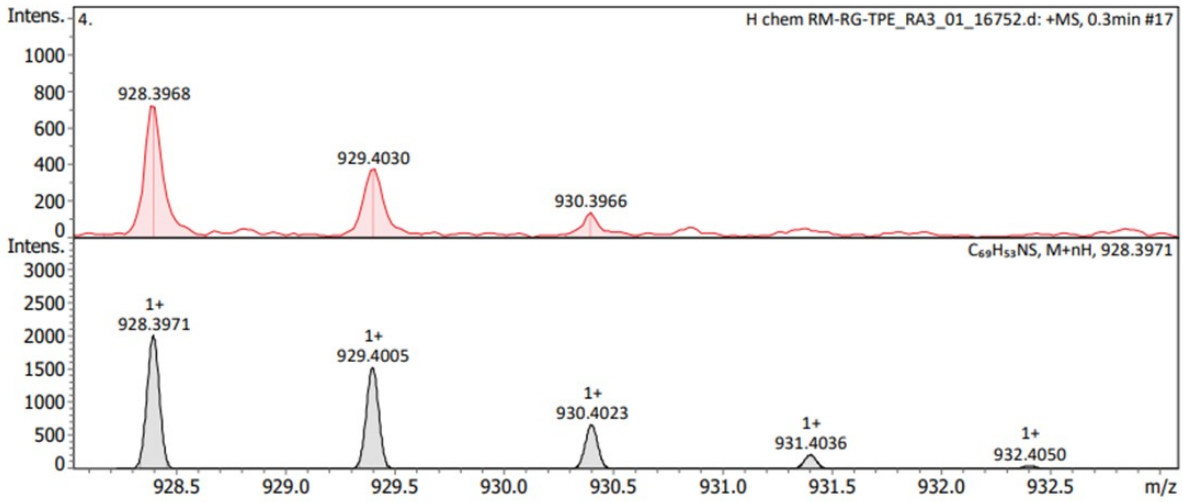

Fig. S17. HRMS of **PTZ-(TPE)$_2$**.

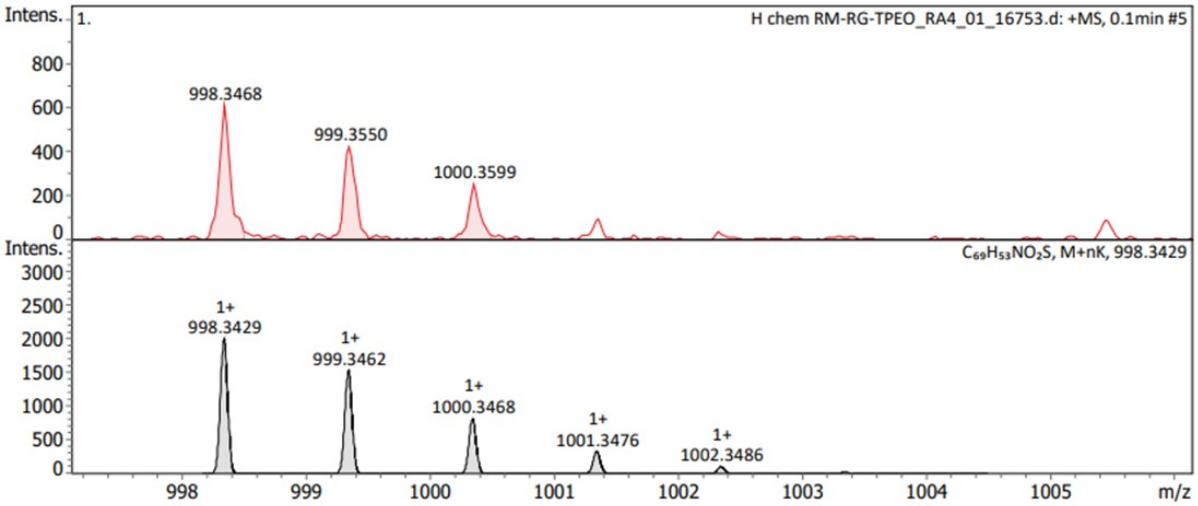

Fig. S18. HRMS of **PTZO$_2$-(TPE)$_2$**.